Journal of Alloys and Compounds 504S (2010) S491–S495

Contents lists available at ScienceDirect

Journal of Alloys and Compounds

journal homepage: www.elsevier.com/locate/jallcom

Effect of cooling rate and Y element on the microstructure of rapidly solidified TiAl alloys

Z.G. Liu [a,b,c], L.H. Chai [c,*], Y.Y. Chen [c]

[a] Key Laboratory of Micro-systems and Micro-structures Manufacturing, Harbin Institute of Technology, Ministry of Education, China
[b] State Key Laboratory of Advanced Welding Production Technology, Harbin Institute of Technology, Harbin 150001, China
[c] School of Materials Science and Engineering, Harbin Institute of Technology, Harbin 150001, China

ARTICLE INFO

Article history:
Received 4 July 2009
Received in revised form
29 December 2009
Accepted 10 February 2010
Available online 18 February 2010

PACS:
81.30.–t
68.55.Nq
68.37.–d

Keywords:
TiAl
Rapid solidification
Microstructure
Cooling rate

ABSTRACT

The influence of cooling rate and rare earth yttrium element on the microstructure of two rapidly solidified TiAl alloys with nominal compositions of Ti–46Al–2Cr–2Nb and Ti–46Al–2Cr–2Nb–1.0Y (at.%) prepared by melt spinning method was studied. The results show that rapid solidification refined and homogenized the microstructure of TiAl alloys, comparing to the conventionally cast mother alloy. A metastable supersaturated α_2 phase was retained to low temperature. With increasing cooling rate, the microstructure is refined more and contains more supersaturated α_2 phases. Y element promotes γ phase nucleation, leading to more γ phase with more Y addition, γ phase was found mainly located at the grain boundaries. Besides the main two phases, supersaturated α_2 and γ, Y-enriched phase was also found in the 1.0 at.% Y containing alloy. The Y-enriched phase distributes as sphere morphology homogeneously in the matrix with a grain size of 20–130 nm. With increasing cooling rate, the amount of Y-enriched phase was decreased, indicating an increasing solubility of Y atom in TiAl alloys.

1. Introduction

TiAl alloy is a kind of attractive high temperature structural materials because of the low density, high strength, and good creep resistance and good oxidization resistance [1]. However, the low ductility at room temperature was the main obstacle for their extensive application. Rapid solidification technique is a kind of method to solve this problem by refining and homogenizing the microstructure [2,3], in particular, the melt spinning method has been used in many kinds of materials [4–6].

The microstructure of rapidly solidified alloys bears strong relationship with the cooling rate. Through controlling the cooling rate one can get the desired structure. There are many processing parameters influencing cooling rate in melt spinning method, such as wheel speed, gas ejection pressure, melt temperature, nozzle–wheel gap, etc. [7], among which the wheel speed is easiest to control. The cooling rate increases linearly with the wheel speed [8]. Therefore, wheel speed was selected for analysing the effect of cooling rate on the microstructure of TiAl alloys.

The rare earth element, especially Y, is an effective element for refining the microstructure, purifying the TiAl alloys and improving the mechanical properties [9–11], which has been considered to be a crucial element in exploring TiAl intermetallics [9]. The influence of Y on the conventionally cast TiAl alloys has been well studied [12]. In the present paper, the rapidly solidified Ti–46Al–2Cr–2Nb and Ti–46Al–2Cr–2Nb–1.0Y alloys were studied. The effects of cooling rate (wheel speed) and addition of Y on the microstructure were studied.

2. Experimental

Two alloys were selected in the present study, Ti–46Al–2Cr–2Nb (at.%) (0Y for short) and Ti–46Al–2Cr–2Nb–1.0Y (at.%) (1Y for short). Pure Ti (>99.99 wt%), Al (>99.99 wt%), Cr (>99.87 wt%) and Nb (>99.87 wt%), Y (>99.99 wt%) were used to produce alloy ingots. The alloys were arc melted under argon atmosphere, and remelted for four times to remove element segregation. The rapidly solidified alloy ribbons were prepared by melt spinning (planar flow cast on a Cu wheel) at different wheel speeds, 15–30 m/s. The obtained ribbons were 2–3 mm wide and 20–50 μm thick. The microstructure of the conventionally cast and the longitudinal section of the rapidly solidified ribbons were observed by optical microscope and scan electron microscope (SEM). Transmission electron microscopic (TEM) observations were carried out in a CM12-PHILIPS (120KV) TEM. Specimens were prepared using an ion-thinning technique (GATAN PIPS 691). X-ray diffraction (XRD) was carried out in a Rigaku D/max-rB X-ray diffractometer using Cu Kα1-radiation at a scan rate of 0.05°/s.

* Corresponding author. Tel.: +86 451 86418802.
E-mail address: lh.chai@163.com (L.H. Chai).

0925-8388/$ – see front matter © 2010 Elsevier B.V. All rights reserved.
doi:10.1016/j.jallcom.2010.02.054

Table 1
The ribbon thickness of rapidly solidified 0Y alloys and 1Y alloys at various wheel speeds.

Alloy composition (at.%)	Wheel speed (m/s)	Thickness (μm)
Ti–46Al–2Cr–2Nb	30	27
	15	50
Ti–46Al–2Cr–2Nb–1.0Y	30	25
	15	36

3. Results and discussion

3.1. The effect of cooling rate and Y on the thickness of rapidly solidified TiAl ribbons

Table 1 shows the thickness of the two alloys at various wheel speeds. The thickness of two alloy ribbons decreases with increasing wheel speed. However, at same wheel speed, the ribbon of 1.0 at.% Y added alloy is thinner. The thickness of the 1Y alloy was found to be inversely proportional to the square root of the wheel speed, which does not work for 0Y alloy. The width of the two alloy ribbons did not vary with cooling rate and Y addition.

The different ribbon thicknesses in the 0Y and 1Y added alloy may be owing to the difference in their thermal physical properties. The rare earth element addition may influence the viscosity of alloy melt. Generally spoken, the viscosity of melt depends on temperature. The higher the temperature, the lower the viscosity. Y addition into TiAl alloy may lower the melt point temperature and decrease the viscosity of alloy melt. In melt spinning process, the melt with lower viscosity improves the flattening of melt puddle, leading to the reduction of thickness of Y added alloy ribbon.

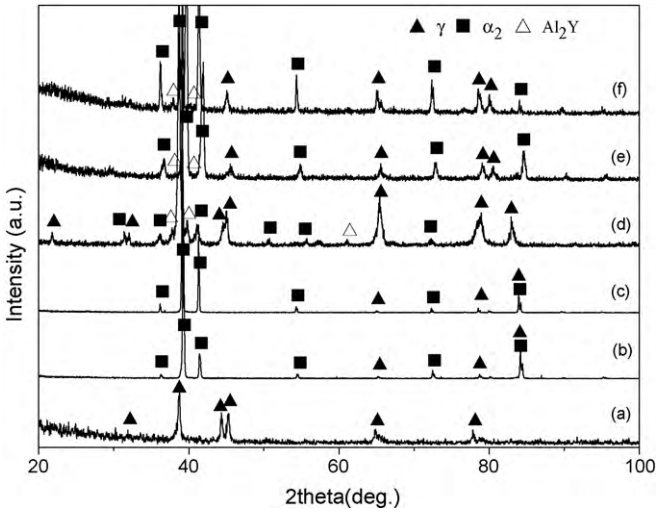

Fig. 1. XRD patterns of Ti–46Al–2Cr–2Nb ((a)–(c)) and Ti–46Al–2Cr–2Nb–1Y ((d)–(f)) alloys at various cooling rates. ((a) and (d)) Conventionally cast mother alloy. ((b) and (e)) Rapidly solidified alloy with a wheel speed of 15 m/s. ((c) and (f)) Rapidly solidified alloy with a wheel speed of 30 m/s.

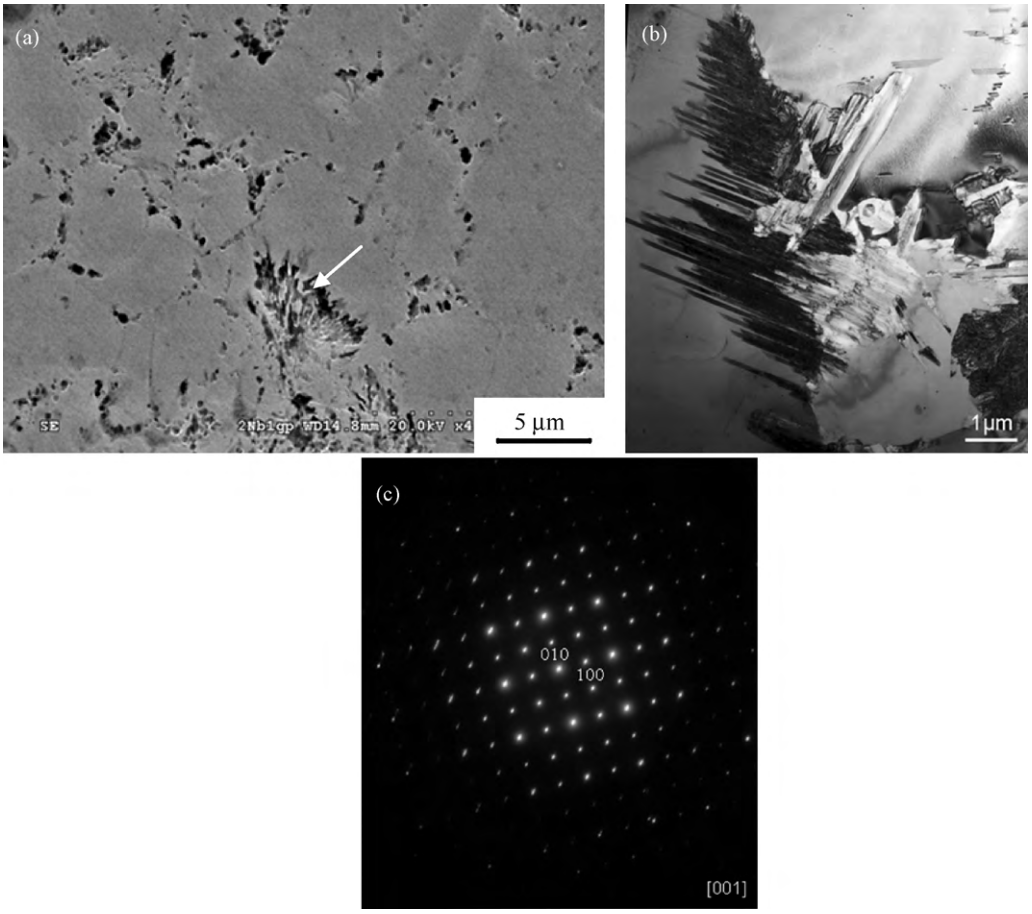

Fig. 2. Microstructure of rapidly solidified Ti–46Al–2Cr–2Nb alloy with lower wheel speed (15 m/s). (a) Lower magnification of the lamellar structure (SEM). (b) Higher magnification of the lamellar γ phase located at the grain boundary (TEM). (c) The corresponding selected area electron diffraction (SAED) pattern of the lamellar structure in (b).

3.2. The effect of cooling rate on the phase composition of 0Y and 1Y alloys

Fig. 1 shows the X-ray diffraction patterns (XRD) of conventionally cast alloys and the rapidly solidified samples of 0Y alloy and 1Y alloy. XRD pattern of the conventionally cast 0Y material [Fig. 1(a)] did not show any prominent peaks of α_2 phase. But in the rapidly solidified samples, α_2 phase became the dominant phase [Fig. 1(b) and (c)]. The volume fraction of α_2 phase was higher in the sample fabricated at higher wheel speed of 30 m/s [Fig. 1(c)] than those at lower wheel speed of 15 m/s [Fig. 1(b)]. XRD pattern of the conventionally cast 1Y alloy [Fig. 1(d)] shows two main phases, γ and α_2. For the rapidly solidified alloy, increasing wheel speed leads to the volume fraction of γ phase decrease. When wheel speed is high, 30 m/s, α_2 phase became the primary phase. A third phase, Al_2Y was also observed in the 1Y alloys produced both by conventionally cast and rapid solidification, with larger amount observed in the conventionally cast one.

3.3. The effect of cooling rate on the microstructure of 0Y alloys

The microstructure of conventionally cast 0Y alloy is full lamellar with a colony size of 100–400 μm. For the 1Y alloy, the microstructure is dendrite with Y rich phase as particle or bar shaped located at grain boundary. The microstructure was refined comparing to the 0Y alloy, but it was still coarse, about 50–100 μm in grain size. More microstructural details of the conventionally alloys can be found in Ref. [13].

Fig. 2 shows the microstructure of rapidly solidified TiAl alloy with a wheel speed of 15 m/s. The dominant phase was supersaturated α_2 with equiaxed grain morphology, and a grain size of about 5–10 μm. Some lamellar grains nucleated at α_2 grain boundary as the arrow indicated in Fig. 2(a) were also observed to grow into one side of the α_2 grain. It was characterized as γ phase by selected area electron diffraction (SAED) [Fig. 2(c)]. High-density stacking faults with the same orientation which results from stresses experienced during solidification of the ribbon were observed in the equiaxed grain, and some located at the front of the lamellar grain growth direction, as shown in Fig. 2(b). Earlier work presented that the stacking faults play an important role in the lamellar phase transformation in TiAl alloys [14–15]. The stacking faults with high energy can provide driving force for γ phase to nucleate and grow.

Fig. 3 shows the microstructure of the 0Y alloy with higher wheel speed (30 m/s). It consists of primary equiaxed supersaturated α_2 grains with a grain size of 1–4 μm and small amount of second phase occasionally found at the grain boundaries or inside the equiaxed grains. The precipitated phase was identified as γ-TiAl phase by selected area electron diffraction in TEM. Comparing to the alloy produced at lower wheel speed, the grain size of α_2 phases was decreased dramatically in the higher wheel speed alloy, while the precipitation was also decreased. Few dislocations or stacking faults were detected in this alloy.

The microstructure of the rapidly solidified 0Y alloys was much refined than the conventionally cast alloy. The fact that there is no apparent contrast difference in the SEM image of the rapidly solidified alloys indicates that rapid solidification homogenized the alloys significantly. The two 0Y rapidly solidified TiAl alloys were

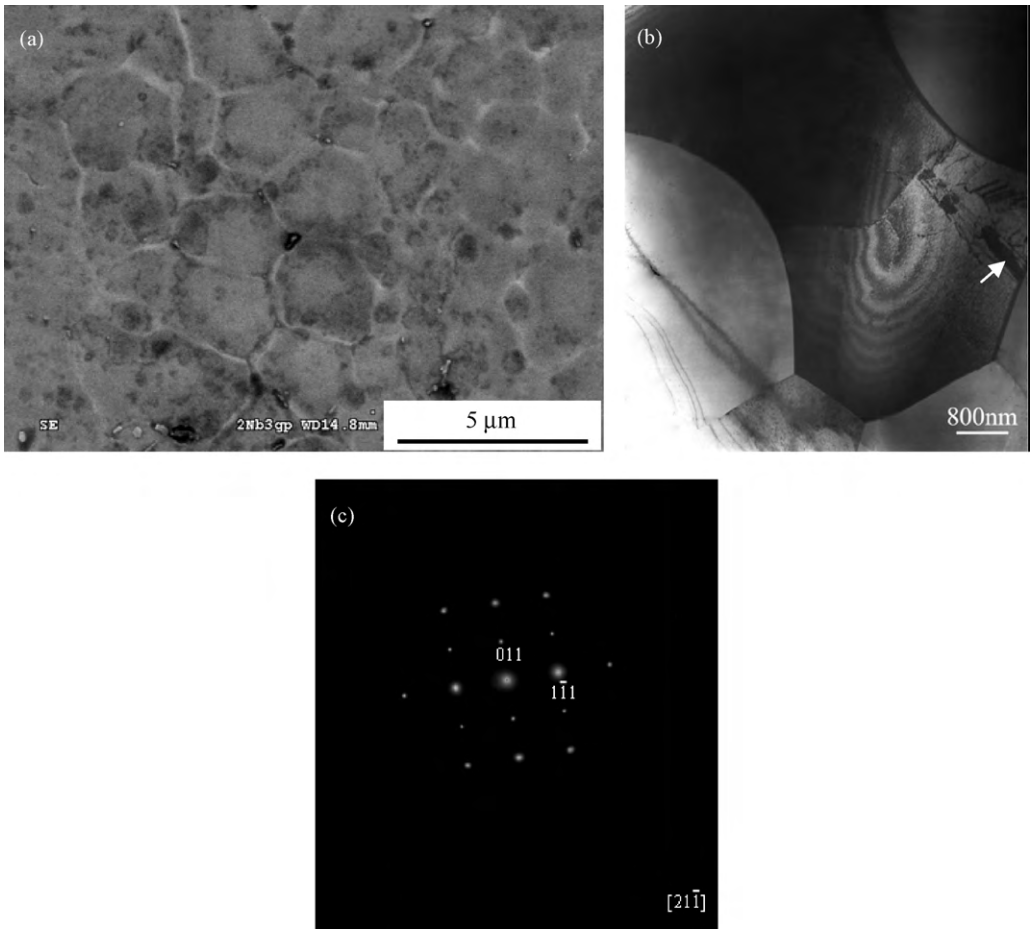

Fig. 3. Microstructure of rapidly solidified Ti–46Al–2Cr–2Nb alloy with higher wheel speed (30 m/s). (a) Lower magnification of the matrix (SEM). (b) The strip like phase inside the equiaxed grain (TEM). (c) The corresponding SAED of the strip like phase in (b).

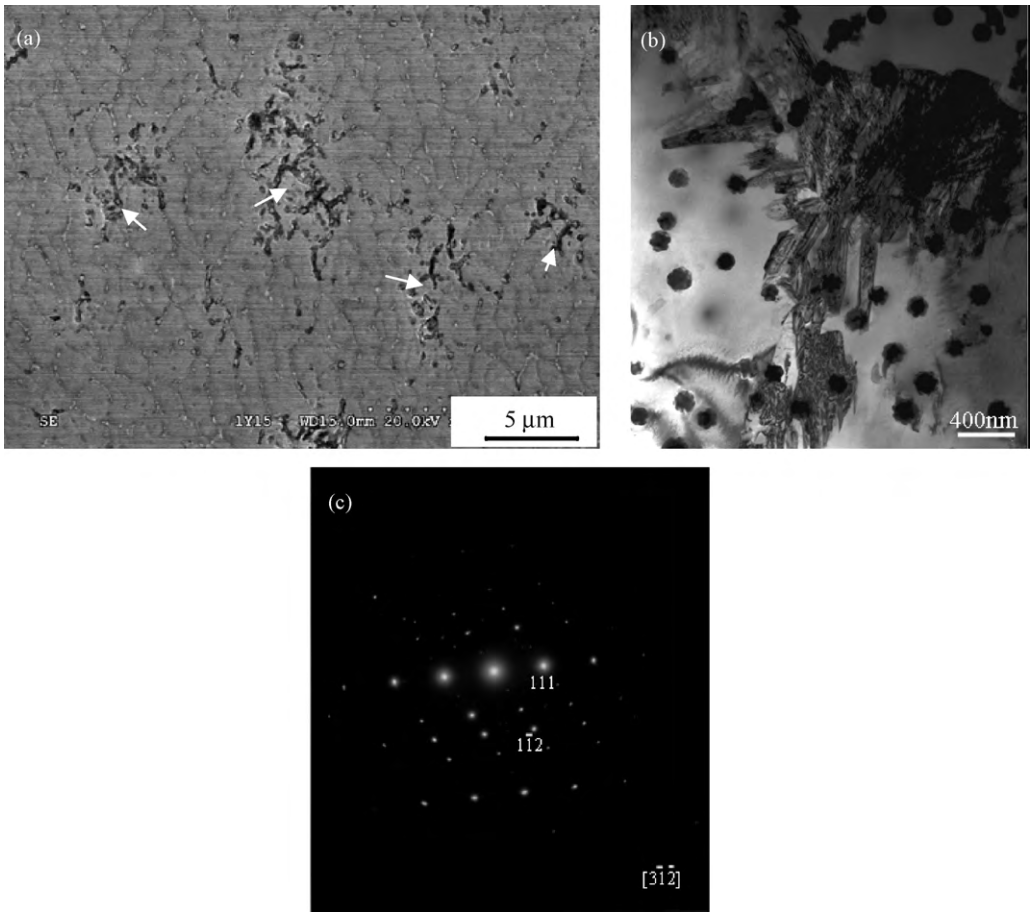

Fig. 4. Microstructural features of the rapidly solidified Ti–46Al–2Cr–2Nb–1.0Y alloy with lower wheel speed (15 m/s). (a) Lower magnification of the matrix (SEM). (b) Lamellar γ phase located at the grain boundary (TEM). (c) The corresponding selected area electron diffraction (SAED) pattern of the lamellar structure in (b).

both solidified directly into the high temperature α phase. The grain size of the primary α phase was controlled by supercooling, the higher cooling rate, the higher supercooling and the smaller grain size. Due to the high cooling rate, the solid-state transformation was suppressed or partly retarded, the high temperature α phase retained and ordered to α_2 phase at lower temperature. When solid phase transformation, such as $\alpha \rightarrow \gamma$ occurs during cooling, the primary phase can be separated by newly formed phase. In the experimental conditions described above, the transformation was very limited so the influence of cooling rate on the nucleation was the main factor. Therefore, the grain size of alloy with higher wheel speed, 30 m/s was smaller than that in the alloy with wheel speed, 15 m/s. The metastable α_2 phase reduces in amount as the cooling rate decreases.

3.4. The effect of cooling rate on the microstructure of 1Y alloys

The microstructure of the rapidly solidified 1Y alloy at lower wheel speed (15 m/s) is shown in Fig. 4. The microstructure consists of equiaxed phase and a small fraction of sphere shaped particles which were speculated as Y-enriched phase embedded in the matrix. A selected area diffraction (SAED) pattern from the matrix which is not shown here indicates that the matrix was α_2 phase. The grain sizes of the equiaxed phase and precipitated particles are about 2–5 μm and 40–130 nm, respectively. Similarly to the 0Y alloy at lower cooling rate, 15 m/s, some lamellar structure grains were also observed locating at α_2 grain boundary, as the arrows indicated in Fig. 4(a) and (b), which was determined as γ phase, but with larger amount presented in this alloy.

The 1Y alloy at a wheel speed of 30 m/s composes of equiaxed structure with grain size of about 0.5–3 μm, as shown in Fig. 5. The selected area diffraction pattern revealed that most of the grains were supersaturated α_2 phase. There was also some massive γ phase formed at grain boundaries and triple points of the parent equiaxed α_2 phase, as shown in Fig. 5(b). The precipitated γ phase was an incompletely ordering phase, owing to the fact that the (0 0 2) and (2 0 0) peaks of γ phase at 2θ of about 45° in XRD pattern overlapped. The growth of γ phase consumed partly of the original coarse α grain, and decreased the grain size of the initial α phase. Comparing to the 1Y alloy with lower cooling rate, a smaller quantity of particles was found in the matrix of this alloy, owing to the high solubility of Y atom at higher cooling rate. The different morphologies of the γ phase at two cooling rate in 1.0Y alloys may partially relate to the difference in Y element solubility.

Comparing the 0Y and 1Y alloy at the same wheel speed, it was found that Y addition greatly refines the microstructure of rapidly solidified TiAl based alloys and the amount of γ phase in the latter alloy is higher at both two cooling rates. It is therefore concluded that Y addition facilitated γ phase formation in Ti–46Al–2Cr–2Nb alloys. The mechanism is regarded to be similar to the Prasad U' statement about the massively transformation of γ phase: the increase in grain size resulted in the reduction of the volume fraction of the massively transformed γ [16]. The solid solubility of Y in TiAl based alloy is very limited, even in the rapidly solidified alloys Y element still cannot solute in the matrix completely. The unsolved Y elements precipitate as small particles, as shown in Fig. 4(b), which acted as nucleate site promoting more α phase nucleation from liquid during solidification process. Thus Y

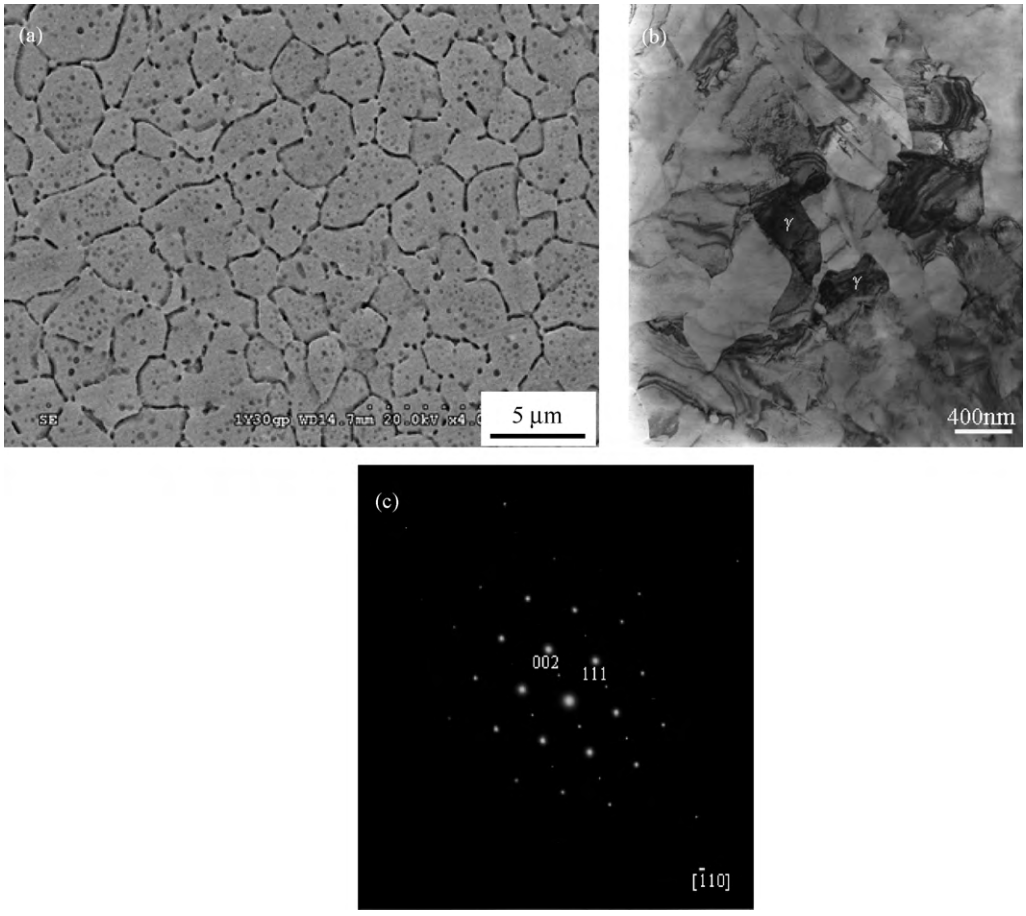

Fig. 5. Microstructure of the rapidly solidified Ti–46Al–2Cr–2Nb–1.0Y alloy with higher wheel speed (30 m/s). (a) Lower magnification of the matrix (SEM). (b) Massive γ phase at grain boundary (TEM). (c) The corresponding SAED pattern in (b).

added into Ti–46Al–2Cr–2Nb alloy refines the original microstructure and the decrease in grain size promotes the increase of the γ phase amount. The solvent Y may also contribute to the increment of γ phase amount by influencing the kinetic of $\alpha \rightarrow \gamma$ phase transformation during subsequent cooling. However, it needs further investigation.

4. Conclusions

In summary, the effect of cooling rate on the microstructure of Ti–46Al–2Cr–2Nb alloys without and with 1.0at.% Y addition was invested.

In the two alloys, the microstructure was refined with increasing cooling rate. Equiaxed metastable α_2 phase was retained to room temperature in rapidly solidified alloys. The higher the cooling rate, the more the amounts of metastable α_2 phase was retained. Some lamellar or massive γ phase was formed at grain boundary in 0Y and 1Y alloy with lower cooling rate, and in 1Y alloy at higher cooling rate, respectively. Rare γ phase was found in 0Y alloy at a wheel speed of 30 m/s. Y addition refined the microstructure of TiAl alloys with the same cooling rate and promoted γ phase formation. Rapid solidification increased the solubility of Y element in TiAl alloys, the higher the cooling rate, the higher the solubility.

Acknowledgement

The financial support from the National Natural Science Fund of China (No. 50674037) is gratefully acknowledged.

References

[1] Y.M. Kim, D.M. Dimiduk, JOM 8 (1991) 40.
[2] E. Frazier, J.S.J. Chen, JOM 44 (1992) 52.
[3] S. Tsukamoto, O. Umezawa, Mater. Sci. Eng. A 223 (1997) 99.
[4] R.A. BuckleyU, S. Kaviani, Mater. Sci. Eng. A 258 (1998) 173.
[5] M.S.F. Lima, P.I. Ferreira, Intermetallics 4 (1996) 85.
[6] E. Karaköse, T. Karaaslan, M. Keskin, O. Uzun, J. Mater. Process. Technol. 195 (2008) 58.
[7] V.I. Tkatch, A.I. Limanovskii, S.N. Denisenko, S.G. Rassolov, Mater. Sci. Eng. A 323 (2002) 9.
[8] W.T. Kim, B. Cantor, Scripta Metall. Mater. 24 (1990) 633.
[9] Y. Wu, S.K. Hwang, Mater. Lett. 58 (2004) 2067.
[10] Y.Y. Chen, B.H. Li, F.T. Kong, J. Alloys Compd. 457 (2008) 265.
[11] P.B. Trivedi, E.G. Baburaj, A. Genc, L. Ovecoglu, S.N. Patankar, F.H. (Sam) Froes, Metall. Mater. Trans. A 33 (2002) 2729.
[12] X.Z. Ma, J. Shen, J. Jia, J. Mater. Sci. Lett. 20 (2001) 2013.
[13] L.H. Chai, Z.G. Liu, Y.Y. Chen, F.T. Kong, S.L. Xiao, Rare Metal Mater. Eng. 37 (2008) 484 (in Chinese).
[14] S.A. Jones, M.J. Kaufman, Acta Metall. Mater. 41 (1993) 387.
[15] S. Zghal, M. Thomas, S. Naka, A. Finel, A. Couret, Acta Mater. 53 (2005) 2653.
[16] U. Prasad, Q. Xu, M.C. Chaturvedi, in: K.J. Hemker, et al. (Eds.), Structural Intermetallics, TMS, Warrendale, PA, 2001, p. 615.